HHS Public Access

Author manuscript

Mol Psychiatry. Author manuscript; available in PMC 2012 December 01.

Published in final edited form as:

Mol Psychiatry. 2012 June ; 17(6): 650–662. doi:10.1038/mp.2011.93.

Dopamine D_4 receptor, but not the ADHD-associated $D_{4.7}$ variant, forms functional heteromers with the dopamine D_{2S} receptor in the brain

Sergio González[1], **Claudia Rangel-Barajas**[2], **Marcela Peper**[3], **Ramiro Lorenzo**[3], **Estefanía Moreno**[1], **Francisco Ciruela**[4], **Janusz Borycz**[5], **Jordi Ortiz**[6], **Carme Lluís**[1], **Rafael Franco**[1,7], **Peter J. McCormick**[1], **Nora D. Volkow**[8], **Marcelo Rubinstein**[3], **Benjamin Floran**[2], and **Sergi Ferré**[5,*]

[1]Centro de Investigación Biomédica en Red sobre Enfermedades Neurodegenerativas, and Department of Biochemistry and Molecular Biology, Faculty of Biology, University of Barcelona, Barcelona, Spain

[2]Departamento de Fisiología, Biofísica y Neurociencias, Centro de Investigación y de Estudios Avanzados del Instituto Politécnico Nacional, México D.F., México

[3]Instituto de Investigaciones en Ingeniería Genética y Biología Molecular, Consejo Nacional de Investigaciones Científicas y Técnicas, Buenos Aires, Argentina

[4]Unitat de Farmacologia, Departament Patologia i Terapèutica Experimental, Facultat de Medicina, Universitat de Barcelona, L'Hospitalet de Llobregat, Barcelona, Spain

[5]National Institute on Drug Abuse, Intramural Research Program, National Institutes of Health, Department of Health and Human Services, Baltimore, MD, USA

[6]Neuroscience Institute and Department of Biochemistry and Molecular Biology, Faculty of Medicine, Universitat Autónoma de Barcelona, Bellaterra, Spain

[7]Centro de Investigación Médica Aplicada, Universidad de Navarra, Pamplona, Spain

[8]National Institute on Drug Abuse, National Institutes of Health, Department of Health and Human Services, Bethesda MD, USA

Abstract

Polymorphic variants of the dopamine D_4 receptor have been consistently associated with attention-deficit hyperactivity disorder (ADHD). However the functional significance of the risk polymorphism (variable number of tandem repeats in exon 3) is still unclear. Here we show that whereas the most frequent 4-repeat ($D_{4.4}$) and the 2-repeat ($D_{4.2}$) variants form functional heteromers with the short isoform of the dopamine D_2 receptor (D_{2S}), the 7-repeat risk allele

[*]Correspondence: Sergi Ferré, National Institute on Drug Abuse, Intramural Research Program, National Institutes of Health, Department of Health and Human Services, 251 Bayview Blvd, Baltimore, MD 21224; phone: 443-740-2647; fax: 443-740-2816; sferre@intra.nida.nih.gov.

Conflict of interest

The authors declare no conflict of interest

($D_{4.7}$) does not. D_2 receptor activation in the D_{2S}-D_4 receptor heteromer potentiates D_4 receptor-mediated MAPK signaling in transfected cells and in the striatum, which did not occur in cells expressing $D_{4.7}$ or in the striatum of knock-in mutant mice carrying the 7 repeats of the human $D_{4.7}$ in the third intracellular loop of the D_4 receptor. In the striatum D_4 receptors are localized in cortico-striatal glutamatergic terminals, where they selectively modulate glutamatergic neurotransmission by interacting with D_{2S} receptors. This interaction shows the same qualitative characteristics than the D_{2S}-D_4 receptor heteromer-mediated MAPK signaling and D_{2S} receptor activation potentiates D_4 receptor-mediated inibition of striatal glutamate release. It is therefore postulated that dysfunctional D_{2S}-$D_{4.7}$ heteromers may impair presynaptic dopaminergic control of corticostriatal glutamatergic neurotransmission and explain functional deficits associated with ADHD.

Keywords

Dopamine receptors; receptor heteromers; ADHD; striatum; glutamate

Introduction

Dopamine D_4 receptors are expressed in the prefrontal cortex (PFC), in GABAergic interneurons and in glutamatergic pyramidal neurons, including their striatal projections.[1–3] D_4 receptors have been implicated in ADHD.[1,4,5] In fact, the PFC and associated fronto-striatal circuits are critical for executive function and are involved in ADHD.[5] The gene encoding the human D_4 receptor contains a large number of polymorphisms in its coding sequence.[4] The most extensive polymorphism is found in exon 3, a region that codes for the third intracellular loop (3IL) of the receptor. This polymorphism consists of a variable number of tandem repeats (VNTR) in which a 48-bp sequence exists as 2- to 11-fold repeats.[7] The three most common variants contain two, four and seven repeats ($D_{4.2}$, $D_{4.4}$ and $D_{4.7}$, respectively). $D_{4.4}$ constitutes the most frequent variant, with a global frequency of 64%, followed by $D_{4.7}$ (21%) and $D_{4.2}$ (8%).[8] Importantly, a high prevalence of the $D_{4.7}$ variant has been demonstrated in children diagnosed with ADHD.[5] Though stimulation of the $D_{4,7}$ variant has been reported to be less potent at inhibiting cAMP than $D_{4.2}$ or $D_{4.4}$,[9] the functional significance of these variants are poorly understood.

Receptor heteromers are becoming the focus of extensive research in the field of G-protein-coupled receptors.[10] A receptor heteromer is currently defined as a macromolecular complex composed of at least two (functional) receptor units with biochemical properties that are demonstrably different from those of its individual components.[10] In some cases, receptor heteromers provide a framework in which to understand the role of receptors with no clear functional significance, and example being the D_3 receptor, which forms heteromers with the D_1 receptor and modifies its function.[11] A recent study showed that in mammalian transfected cells the long isoform of the D_2 receptor (D_{2L}) heteromerizes with the three main D_4 receptor variants, $D_{4.2}$, $D_{4.4}$. and $D_{4.7}$.[12] Interestingly, results from the same study suggested that $D_{4.7}$ was less effective in forming heteromers with D_{2L} receptors.[12] In view of the reported evidence of predominant co-localization of D_4 receptors with the short isoform of the D_2 receptor (D_{2S}) in cortico-striatal glutamatergic terminals,[2,3,13] we first

investigated if any of the three main human variants of the D_4 receptor could interact both physically and functionally with D_{2S}. By using the Bioluminescence Resonance Energy Transfer (BRET) technique, here we show evidence for the formation of heteromers between D_{2S} and $D_{4.2}$ and $D_{4.4}$ variants of the D_4 receptor. In contrast, the $D_{4.7}$ variant failed to form heteromers with the D_{2S} receptor. In transfected cells we found a biochemical property of the D_{2S}-D_4 receptor heteromer, which consists of the ability of D_{2S} receptor activation to potentiate D_4 receptor-mediated MAPK signaling. A similar result was observed in striata from wild-type mice, a species that expresses D_4 receptors with a short 3IL comparable to human $D_{4.2}$. In contrast, potentiation of D_4 receptor-mediated MAPK signaling was not observed in transfected cells expressing $D_{4.7}$ or in striata taken from *knock-in* mice carrying a humanized 7 repeat intracellular loop identical to that found in human $D_{4.7}$. Finally, analyzing neurotransmitter release in striatal slices and with *in vivo* microdialysis in rats, evidence was obtained for a key role of D_2-D_4 receptor interaction in the modulation of striatal glutamatergic neurotransmission.

Materials and methods

Fusion Proteins and Expression Vectors

The synthetic cDNAs for the human $D_{4.2}$, $D_{4.4}$ and, $D_{4.7}$ receptor gene (kindly provided by T.P. Sakmar, Rockefeller University, USA) were amplified using sense oligonucleotide primer (5´- TCAACGGGACTTTCCAAAATGT-3´) and antisense primer (5´ CTCCGAGATCAACTTCTGCTCGCTTCGGTTACCC-3´) resulting in a cDNA fragment of 200 bp. A second product was generated using the sense oligonucleotide primer (5´-AAGTTGATCTCGGAGGAAGATACAGCAGATGCAG-3´) and antisense primer (5´-GCGAATTCGCAGCAAGCACGTAGAGCCTTACG-3´) resulting in a cDNA fragment of 1500 bp. Equimolar quantities of both fragments were used to produce a third product corresponding to the myc-$D_{4.2}$, myc-$D_{4.4}$ or myc-$D_{4.7}$ tagged gene using the sense primer (5´- GTGCTCGAGCACCATGGGTAACCGAAGCACAG-3´) and antisense primer without its stop codon (5´- GCGAATTCTCAGCAGCAAGCACGTAGAGCCTTACG-3´) harbouring unique XhoI and EcoRI restriction sites, respectively. The fragments were then subcloned in-frame into XhoI/EcoRI sites of the pcDNA3.1 vector (Invitrogen). Next, the human cDNAs for the adenosine A_1 receptor and dopamine $D_{4.2}$, $D_{4.4}$, $D_{4.7}$ and D_{2S} receptors, cloned in *pcDNA3.1* were amplified without their stop codons using sense and antisense primers harboring unique XhoI and EcoRI sites to clone A_1, $D_{4.2}$, $D_{4.4}$ and $D_{4.7}$ receptors in the RLuc and the YFP corresponding vectors, and HindIII and BamHI to clone D_{2S} in the RLuc and the YFP corresponding vectors. The mouse cDNAs for the D_4 and D_{2S} receptors, cloned in pCMV-SPORT6 (ATCC, Manassas, USA) and pReceiver-M16 vectors respectively (GeneCopoeia, Rockville, USA), were amplified without their stop codons using sense and antisense primers harboring unique XhoI and EcoRV sites to clone D_4 receptor in the RLuc corresponding vector, and XhoI and KpnI to clone D_{2S} receptor in the RLuc and the YFP corresponding vectors. The amplified fragments were subcloned to be in-frame into restriction sites of the multiple cloning sites of EYFP-N3 vector (enhanced yellow variant of YFP; Clontech, Heidelberg, Germany) or the mammalian humanized pRluc-N1 vectors (Perkin-Elmer, Waltham, MA, USA) to give the plasmids that express the receptors fused to either Rluc or YFP on the C-terminal end of the receptor ($D_{4.2}$-RLuc,

$D_{4.4}$-RLuc, $D_{4.7}$-Rluc, D_{2S}-RLuc and A_1-RLuc or D_{2S}-YFP, $D_{4.7}$-YFP, and D_1-YFP, respectively). All constructs were verified by nucleotide sequencing and the fusion proteins are functional and expressed at the membrane level (see Results).

Cell Culture and transient transfection

Human embryonic kidney (HEK)-293T cells were grown in Dulbecco's modified Eagle's medium (DMEM) (Gibco Paisley, Scotland, UK) supplemented with 2 mM L-glutamine, 100 U/ml penicillin/streptomycin, and 5% (v/v) heat inactivated Foetal Bovine Serum (FBS) (all supplements were from Invitrogen, Paisley, Scotland, UK). CHO cell lines were maintained in α-MEM medium without nucleosides, containing 10% fetal calf serum, 50 μg/ml penicillin, 50 μg/ml streptomycin and 2 mM L-glutamine (300 μg/mL). Cells were maintained at 37°C in an atmosphere of 5% CO_2, and were passaged when they were 80–90% confluent, twice a week. HEK-293T or CHO cells growing in 6-well dishes or in 25 cm^2 flasks were transiently transfected with the corresponding fusion protein cDNA by the PEI (PolyEthylenImine, Sigma, Steinheim, Germany) method as previously described.[14]

Immunostaining

For immunocytochemistry, HEK-293T cells were grown on glass coverslips and transiently transfected with 1 μg of cDNA corresponding to human $D_{4.2}$-RLuc, $D_{4.4}$-RLuc or $D_{4.7}$-RLuc and 0.5 μg of cDNA corresponding to human D_{2S}-YFP or 0.8 μg of cDNA corresponding to mouse D_4-RLuc and 0.5 μg of cDNA corresponding to mouse D_{2S}-YFP. After 48h of transfection cells were fixed in 4% paraformaldehyde for 15 min and washed with phosphate-buffered saline contraining 20 mM glycine to quench the aldehyde groups. After permeabilization with phosphate-buffered saline containing 0.05% Triton X-100 for 15 min, cells were treated with phosphate-buffered saline containing 1% bovine serum albumin. After 1 h at room temperature, cells were labeled with the primary rabbit monoclonal anti-human D_4 receptor (1/10.000, Abcam, Cambridge, UK) or with the primary goat polyclonal anti-D_4 receptor (1/500, Santa Cruz Biotechnology) for 1 h, washed and stained with the secondary antibody Cy3 anti-rabbit (1/200, Jackson ImmunoResearch, Baltimore, PA) or with the secondary antibody Cy3 anti-goat (1/200, Jackson ImmunoResearch, Baltimore, PA). The D_{2S}-YFP construct was detected by its fluorescence properties. Samples were rinsed and observed in an Olympus confocal microscope.

BRET assay

HEK-293T cells were co-transfected with a constant amount of cDNA encoding for the receptor fused to Rluc and with increasingly amounts of cDNA encoding to the receptor fused to YFP to measure BRET as previously described (23). Both fluorescence and luminescence for each sample were measured before every experiment to confirm similar donor expressions (approximately 100,000 bioluminescence units) while monitoring the increase in acceptor expression (2000 to 20,000 fluorescence units). The relative amounts of BRET acceptor are expressed as the ratio between the net fluorescence of the acceptor and the luciferase activity of the donor being the net fluorescence the fluorescence of the acceptor minus the fluorescence detected in cells only expressing the donor. The BRET ratio is defined as [(emission at 510–590)/(emission at 440–500)] - Cf, where Cf corresponds to (emission at 510–590)/(emission at 440–500) for the D_4-RLuc or D_{2S}-Rluc constructs

expressed alone in the same experimental conditions. Curves were fitted by using a non-linear regression equation, assuming a single phase with GraphPad Prism software (San Diego, CA, USA).

Generation of knockin mutant mice carrying human expansions in the 3IL of the D_4 receptor

A targeting vector was designed such that coding sequences of the 3IL of mouse *Drd4* were replaced by human ortholog sequences corresponding to the most frequent 7-VNTR human variant allele (see Figure 4). The vector included a selectable PGK-*neo* cassette, flanked by two loxP sites, placed just downstream of *Drd4* polyadenylation site and an HSV-thymidine kinase cassette placed at one of the extremes of the targeting vector to select for the absence of random integrations. A long and short arm of *Drd4* homology were inserted flanking the swapped sequence and the selectable marker, respectively. The linearized vector was used to electroporate hybrid 129svev/C57BL/6 ES cells (inGenious Targeting Laboratory Inc., USA) and homologous recombinant clones were selected in the presence of G418 and gancyclovir. Two selected clones carrying the human 7-VNTR were used to microinject C57BL/6J blastocysts and one high percentage chimeric male mouse was used to produce heterozygote *Drd4*$^{+/7repeat.neo}$ mice. The neo cassette was excised from the recombinant allele by crossing mutant mice with transgenic mice expressing Cre recombinase from an EIIa promoter (Jackson Laboratories, USA; Cat. No. 003724). The resulting heterozygote *Drd4*$^{+/7repeat}$ ($D_{4.7}$ knockin) mice were successively bred to C57BL/6J mice to obtain a congenic heterozygote strain (n=10) that was used to establish a breeding colony. Homozygous $D_{4.7}$ knockin mice and their wild-type littermates were used for the experiments. Knockin animals were characterized as indicated in Figure 4.

Mouse striatal slices preparation

Mice were housed five per cage in a temperature (21 ± 1°C) and humidity-controlled (55 ± 10%) room with a 12:12 hours light/dark cycle (light between 08:00 and 20:00 hours) with food and water *ad libitum*. All animal procedures were conducted according to standard ethical guidelines (National Institutes of Health Animal care guidelines and European Communities Council Directive 86/609/EEC) and approved by the Local Ethical and Animal Care Committees. Transgenic mice and litter-mattes were decapitated with a guillotine and the brains were rapidly removed and placed in ice-cold oxygenated (O_2/CO_2:95%/5%) Krebs-HCO3$^-$ buffer (124 mM NaCl, 4 mM KCl, 1.25 mM NaH_2PO_4, 1.5 mM $MgCl_2$, 1.5 mM $CaCl_2$, 10 mM glucose and 26 mM $NaHCO_3$, pH 7.4). The brains were sliced at 4°C in a brain matrix (Zivic Instruments, Pittsburgh, PA, USA) into 0.5 mm coronal slices. Slices were kept at 4°C in Krebs-HCO_3^- buffer during the dissection of the striatum. Each slice was transferred into an incubation tube containing 1 ml of ice-cold Krebs-HCO_3^- buffer. The temperature was raised to 23°C and after 30 min, the media was replaced by 2 ml Krebs-HCO_3^- buffer (23°C).

ERK phosphorylation assay

Striatal slices from transgenic mice and litter-mattes were incubated under constant oxygenation (O_2/CO_2:95%/5%) at 30°C for 4–5 h in an Eppendorf Thermomixer (5 Prime,

Inc., Boulder, CO, USA) with Krebs-HCO_3^- buffer. The media was replaced by 200 μl of fresh Krebs-HCO_3^- buffer and incubated for 30 min before the addition of ligands. Transfected CHO cells were cultured in serum-free medium for 16 h before the addition of the indicated concentration of ligands for the indicated time. Both, cells and slices were lysed in ice-cold lysis buffer (50 mM Tris- HCl pH 7.4, 50 mM NaF, 150 mM NaCl, 45 mM β-glycerophosphate, 1% Triton X-100, 20 μM phenylarsine oxide, 0.4 mM $NaVO_4$ and protease inhibitor cocktail). Cellular debris was removed by centrifugation at 13,000 g for 5 min at 4°C and protein was quantified by the bicinchoninic acid method using bovine serum albumin dilutions as standard. To determine the level of ERK1/2 phosphorylation, equivalent amounts of protein (10 μg) were separated by electrophoresis on a denaturing 10% SDS-polyacrylamide gel and transferred onto PVDF-FL membranes. Odyssey blocking buffer (LICOR Biosciences, Lincoln, Nebraska, USA) was then added and membranes were blocked for 90 min. Membranes were then probed with a mixture of a mouse anti-phospho-ERK 1/2 antibody (1:2500, Sigma, Steinheim, Germany) and rabbit anti-ERK 1/2 antibody (1:40000, Sigma) for 2–3 h. Bands were visualized by the addition of a mixture of IRDye 800 (anti-mouse) antibody (1:10000, Sigma) and IRDye 680 (anti-rabbit) antibody (1:10000, Sigma) for 1 h and scanned by the Odyssey infrared scanner (LICOR Biosciences, Lincoln, Nebraska, USA). Bands densities were quantified using the scanner software and exported to Excel (Microsoft, Redmond, WA, USA). The level of phosphorylated ERK1/2 isoforms was normalized for differences in loading using the total ERK protein band intensities.

In vivo microdialysis in rat striatum

Male Sprague-Dawley rats (Charles River Laboratory, Wilmington, MA, USA), weighing 300–350 g were used. Concentric microdialysis probes with 2-mm long dialysis membranes were prepared as described previously.[15] Animals were anesthetized with Equithesin (NIDA Pharmacy, Baltimore, MD, USA) and microdialysis probes were implanted in the ventral striatum (core of the nucleus accumbens); coordinates with respect to bregma: A 1.7, L +1.2 and V -7.6 mm. The experiments were performed on freely moving rats 24 h after the probe implantation. A Ringer solution (in mmol/l) of 147 NaCl, 4 KCl, and 2.2 $CaCl_2$ was pumped through the dialysis probe at a constant rate of 1 μl/min. After a washout period of 90 min, samples were collected at 20-min intervals and split into two fractions of 10 μL, to separately measure glutamate and dopamine contents. Each animal was used to study the effect of one treatment by local administration (perfusion by reverse dialysis) of the D_4 receptor agonist RO-10-5824 or the D_4 receptor antagonist L-745,870. At the end of the experiment, rats were killed with an overdose of Equithesin and methylene blue was perfused through the probe. The brain was removed and placed in a 10% formaldehyde solution, and coronal sections were cut to verify the probe location. Dopamine content was measured by reverse high-performance liquid chromatography (HPLC) coupled to an electrochemical detector, as described in detail previously.[15] Glutamate content was measured by HPLC coupled to a flourimetric detector, as described before.[16] The limit of detection (which represents three times baseline noise levels) for dopamine and glutamate was 0.5 and 50 nM, respectively. Dopamine and glutamate values were transformed as percentage of the mean of the three values before the stimulation and transformed values were statistically analyzed with one-way repeated measures ANOVA followed by Newman-

Keuls tests, to compare glutamate and dopamine values of the samples obtained after drug perfusion with those obtained just before drug perfusion.

Neurotransmitter release in rat striatal slices

Rat brain slices were obtained from male Wistar rats weighing 180–220 g. After rapid sacrifice of the rat, the brain was immersed in oxygenated ice-cold artificial cerebrospinal fluid (ACSF) solution, and coronal brain slices (300 μm thick) were obtained with a vibratome. The striatum (caudate-putamen and nucleus accumbens) was microdissected under a stereoscopic microscope and the slices were incubated for 30 min at 37°C in ACSF (in mM: NaCl 118.25, KCl 1.75, $MgSO_4$ 1, KH_2PO_4 1.25, $NaHCO_3$ 25, $CaCl_2$ 2, and D-glucose 10.), gassed continuously with O_2/CO_2 (95:5, v/v). For GABA release, the slices were then incubated for 30 min with 8 nM [^{3}H]GABA in 2 ml solution containing 10 μM aminooxyacetic acid (to inhibit GABA transaminase, thus preventing degradation of the labeled GABA). At the end of this period, excess radiolabeled compound was removed by washing twice with ACSF containing, in addition to aminooxyacetic acid and 10 μM nipecotic acid (to prevent the reuptake of the released [^{3}H]GABA). Both compounds were present in the perfusion solution for the rest of the experiment. For dopamine release, the slices were labeled with 77 nM [^{3}H]dopamine in Krebs–Henseleit solution containing 10 μM pargyline, 0.57 mM ascorbic acid and 0.03 mM EDTA, which were present in the solutions for the rest of the experiment. For glutamate release, the tissues were incubated for 30 min with 100 nM [^{3}H]glutamate in 2 ml of artificial CSF containing 200 μM aminooxyacetic acid (to inhibit glutamate decarboxylase and prevent the conversion of glutamate to GABA) and 200 μM dihydrokainic acid (to prevent the uptake of [^{3}H]glutamate by astrocytes). Dihydrokainic acid was present in the medium only during the incubation period. At the end of this period, the excess radiolabeled compound was removed by washing twice with artificial CSF. Methods for measuring [^{3}H]neurotransmitter release and data analysis used in the present work were the same as those described previously.[17,18] The slices were apportioned randomly between the chambers (usually three slices per chamber) of a superfusion system (volume of each chamber 80 μl; 20 chambers in parallel) and perfused with the artificial CSF at a flow rate of 0.5 ml/min for 1 h. Basal release of [^{3}H]neurotransmitter was measured by collecting 4 fractions of the superfusate (total volume 2 ml) before depolarizing the slices with a solution in which the [K^+] was raised to 25 mM. The composition of the high K^+ solution was (in mM): NaCl 101.25, KCl 23.75, $MgSO_4$ 1, KH_2PO_4 1.25, $NaHCO_3$ 25, $CaCl_2$ 2 and D-glucose 10. Six more fractions were collected in the high K^+ medium. All drugs were added to the medium at fraction 2, before changing the superfusion to the high K^+ medium, to explore effects on basal release. To determine the total amount of tritium remaining in the tissue, the slices were collected, treated with 1 ml of 1 M HCl and allowed to stand for 1 h before adding the scintillator. The [^{3}H]neurotransmitter release was expressed initially as a fraction of the total amount of tritium remaining in the tissue. The effect of drugs on the basal release of [^{3}H]neurotransmitter was assessed by comparing the fractional release in fraction 2 (immediately before exposure of the tissue to the drug) and fraction four (immediately prior to exposure to 25 mM of K^+), using Student's paired *t* test. Changes in depolarization-induced [^{3}H]GABA release by drugs and treatments, were assessed by comparing the area under the appropriate release curves between the first and last fractions collected after the

change to high K^+. The significance of drug effects was assessed by one-way ANOVA and Tukey-Kramer test, using Prism Graph Pad Software 4.0, (Graph Pad Software, San Diego CA, USA). To obtain an unbiased estimate of IC_{50} values, concentration-response data were fitted by non-linear regression using the same software.

Statistical Analysis

Statistical analyses were performed with Prism Graph Pad Software 4.0, (Graph Pad Software, San Diego CA, USA). See above and figure legends for details.

Results

D_{2S} and D_4 receptors form heteromers in transfected cells

BRET experiments were performed where one of the receptor is fused to the bioluminescent protein *Renilla Luciferase* (RLuc) and the other receptor is fused to a yellow fluorescent protein (YFP). The fusion proteins were functional (Supplementary Figure 1) and expressed at the membrane level (Figure 1c). Clear BRET saturation curves were obtained in cells expressing $D_{4.2}$-RLuc or $D_{4.4}$-RLuc receptors and increasing amounts of D_{2S}-YFP (Figure 1a), but not in cells expressing $D_{4.2}$-RLuc or $D_{4.4}$-RLuc receptors and increasing amounts of D_1-YFP (Figure 1a), indicating that the $D_{4.2}$ and the $D_{4.4}$ form heteromers with D_{2S} but not with D_1 receptors. Interestingly, in cells expressing the $D_{4.7}$-Rluc variant and D_1-YFP or D_{2S}-YFP (Figure 1a) low linear BRET was detected, which was qualitatively similar to the results obtained with the negative control, with adenosine A_1-RLuc and D_{2S}-YFP receptors (Figure 1a). This result was not due to the particular BRET donor and acceptor chosen, as low and linear BRET were obtained when we swapped the fused proteins, i.e., in cells co-expressing D_{2S}-Rluc and $D_{4.7}$-YFP (Figure 1a). These results strongly suggest that the human $D_{4.7}$ polymorphic variant does not form heteromers with the human D_{2S} receptor or if heteromers are formed, the fusion proteins are not properly oriented or are not within proximity to allow energy transfer (less than 10 nm). One way to test if the receptors are indeed forming heteromers in such a way that impedes energy transfer is to titrate one receptor in the presence of the heteromer and look for changes in the BRET signal. In BRET displacement experiments, $D_{4.2}$, but not $D_{4.7}$ receptors were able to compete with $D_{4.4}$-Rluc and alter heteromer formation with D_{2S}-YFP (Figure 1b), meaning that $D_{4.2}$ and $D_{4.4}$, but not $D_{4.7}$ receptors use the same molecular determinants to establish intermolecular interactions with D_{2S} receptor and strongly suggesting that $D_{4.7}$ receptors are unable to form heteromers with D_{2S}.

D_{2S}-D_4 receptor heteromer signals through MAPK

To investigate the function of the D_{2S}-D_4 receptor heteromer, MAPK signaling (ERK1/2 phosphorylation) was determined. RO-10-5824 and quinelorane, selective D_4 and $D_{2/3}$ receptor agonists respectively,[19,20] selectively stimulated MAPK in cells transfected with D_4 or D_{2S} receptors, respectively (Supplementary Figure 2). Dose-response experiments with RO-10-5824 showed no significant differences between cells transfected with $D_{4.2}$, $D_{4.4}$ or $D_{4.7}$ receptors (Supplementary Figure 2). However, in co-transfected cells, stimulation of D_{2S} receptors potentiated D_4 receptor-mediated MAPK activation, but not the other way around. Importantly, this functional interaction only occurred in cells transfected with D_{2S}

and $D_{4.2}$ or $D_{4.4}$, but not in cells expressing $D_{4.7}$ receptors (Figure 2). Since disruption of D_{2S}-D_4 receptor heteromers (by substituting $D_{4.2}$ or $D_{4.4}$ with the $D_{4.7}$ variant) is associated with the loss of the D_{2S}-D_4 receptor interaction at the MAPK level, this interaction constitutes a specific biochemical property of the D_{2S}-D_4 receptor heteromer and can be used as a biochemical fingerprint to detect the heteromer in native tissues.[10]

D_{2S}-D_4 receptor heteromers in the mouse brain

D_4 receptors are preferentially expressed in limbic areas and the PFC, where they can be found in interneurons and also projecting neurons.[1] In cortico-striatal neurons D_4 receptors have also been localized at their nerve terminals,[2,3] where they can co-localize with D_{2S} receptors.[13] We therefore investigated the existence of D_{2S}-D_4 receptor heteromers in the striatum. Biophysical techniques cannot be easily applied in native tissues, but indirect methods can be used, such as the identification of a biochemical property of the heteromer (biochemical fingerprint).[10] In this case, the biochemical fingerprint would be the potentiation by D_{2S} receptor activation of D_4 receptor-mediated MAPK activation, which should not occur with the human $D_{4.7}$ variant. Prior to these experiments with mouse brain, we demonstrated by BRET saturation experiments in transfected cells that the mouse D_{2S} receptor forms heteromers with the mouse D_4 receptor (which has an amino acid sequence in the 3IL similar to that from the human $D_{4.2}$). Mouse fusion proteins were expressed in the plasma membrane of transfected cells (Figure 3a) and shown to be functional (Supplementary Figure 3). Like the human receptors, mouse D_{2S} receptors were found to form heteromers with mouse D_4 receptors and also with human $D_{4.4}$ receptors, but not with human $D_{4.7}$ receptors (Figure 3b). Furthermore, it was also shown that, in co-transfected cells, stimulation of the mouse D_{2S} receptor potentiates the effect of the mouse D_4, but not the human $D_{4.7}$, on MAPK signaling (Figures 3c,d). This result was not reciprocal (Supplementary Figure 4) and mirrors the results obtained with human D_4 and D_{2S} receptors (Figure 2). We next analyzed the effects of D_2 and D_4 receptor agonists on MAPK signaling on striatal slices taken from knock-in mice carrying the 7 repeats of the human $D_{4.7}$ in replacement of the mouse region and from wild-type littermates (Figure 4). Neither quinelorane nor RO-10-5824 induced a significant ERK1/2 phosphorylation in striatal slices of wild-type mice when administered alone, but co-administration of both agonists produced a significant dose-dependent effect with an increase of up to four fold (Figure 3e). This synergistic interaction between D_2 and D_4 receptors, which constitutes the biochemical fingerprint of the D_{2S}-D_4 receptor heteromer, was completely absent in the $D_{4.7}$ mutant mouse (Figure 3e), confirming both the existence of D_{2S}-D_4 receptor heteromers and the absence of functional interactions between D_2 and $D_{4.7}$ receptors in the brain.

D_2-D_4 receptor interactions modulate striatal glutamate release

To investigate the functional significance of D_4 receptor activation we determined D_4 receptor-mediated modulation of striatal glutamate release by *in vivo* microdialysis in freely moving rats. The local perfusion of the D_4 receptor agonist RO-10-5824 in the ventral striatum (in the nucleus accumbens) produced a dose-dependent decrease in the striatal extracellular concentration of glutamate and a concomitant increase in the extracellular concentration of dopamine (Figure 5a and 5b), which were counteracted by co-perfusion with the selective D_4 receptor antagonist L-745,870 (which was inactive when perfused

alone) (Figure 5a, 5b and 5c). These results suggest that inhibitory D_4 receptors are located in glutamatergic terminals, whose activation decreases basal striatal glutamate release. The increase in dopamine concentration can best be explained by a decreased activation of striatal GABAergic efferent neurons that tonically inhibit dopaminergic mesencephalic neurons. This interpretation could be confirmed in experiments with striatal slices, where dopamine should not be modified due to the interruption of the striatal-mesencephalic loop. In fact, in slices of dorsal or ventral rat striatum, the D_4 receptor agonist RO-10-5824 decreased K^+-induced glutamate release, an effect that was counteracted by the selective D_4 receptor antagonist L-745,870, but did not change dopamine or GABA release (Figure 6), indicating that striatal D_4 receptors selectively and locally modulate glutamate release. This role of D_4 receptors in the striatum can also explain previous results obtained with D_4 receptor KO mice, which show an increase and decrease in the striatal extracellular concentration of glutamate and dopamine, respectively.[21,22]

As mentioned before, there is evidence for co-localization of both D_2 and D_4 receptors in cortico-striatal glutamatergic terminals[2,3,13] and previous studies have demonstrated that presynaptic D_2-like receptors play an inhibitory role in the modulation of striatal glutamate release.[13,23] However, since those studies did not use selective compounds, they could not distinguish between effects due to D_2 or D_4 receptor stimulation. Therefore, in this study we tested the effect of quinelorane alone and in combination with RO-10-5824 on glutamate release in rat striatal slices. To eliminate endogenous dopamine, rats were treated with reserpine, and the experiments performed in the presence of the D_1-like receptor antagonist SCH-23390. Quinelorane significantly decreased K^+-induced glutamate release whereas the co-application of quinelorane with RO-10-5824 showed a more significant effect (Figure 7a). Dopamine strongly decreased K^+-induced glutamate release, an effect partially counteracted by the D_2 receptor antagonist L-741,626 or by the D_4 receptor antagonist L-745,870, but completely counteracted by the simultaneous application of both antagonists (Figure 7b). In agreement with the reported higher *in vitro* affinity of D_4 versus D_2 receptor for dopamine,[24] the IC_{50} of dopamine-mediated inhibition of K^+-induced glutamate release was significantly higher in the presence of the D_4 receptor antagonist (D_2-mediated effect) than in the presence of the D_2 receptor antagonist (D_4-mediated effect) (Figure 7b). Finally, and more importantly, the D_2 receptor agonist quinelorane synergistically potentiated the inhibitory effect of the D_4 receptor agonist RO-10-5824 on K^+-induced glutamate release (significant decrease in IC_{50} value) (Figure 7c), but not the other way around (Figure 7d). These results therefore show the same kind of D_2-D_4 receptor interaction demonstrated by D_{2S}-D_4 receptor heteromers in transfected cells with MAPK signaling. Our combined *in vitro* and *in vivo* data strongly suggest that D_{2S}-D_4 receptor heteromers are likely to play a key role in dopamine-mediated modulation of striatal glutamate release

Discussion

The present study shows that dopamine D_{2S} and $D_{4.2}$ or $D_{4.4}$ receptors, but not the ADHD-associated human $D_{4.7}$ variant, form functional heteromers in transfected cells and in the rodent brain. Co-stimulation of D_{2S} and D_4 receptors in the D_{2S}-D_4 receptor heteromer has a synergistic effect on MAPK signaling, which could be demonstrated in transfected cells and in the mouse striatum, but not in cells expressing $D_{4.7}$ or in the striatum of a mutant mouse

carrying the 7 repeats of the human $D_{4.7}$ in the 3IL of the D_4 receptor. These results provide a significant functional difference of one of the human receptor variants, $D_{4.7}$, compared to the $D_{4.2}$ and $D_{4.4}$ variants, which can have important implications for the understanding of the pathogenesis of ADHD. Importantly, we also demonstrated, for the first time, that D_{2S}-D_4 receptor interactions modulate striatal glutamate release suggesting that the D_{2S}-D_4 receptor heteromer allows dopamine to fine-tune glutamate neurotransmission.

The molecular mechanism involved in preventing heteromer formation between D_{2S} and $D_{4.7}$ receptors is not yet known. Indeed, the control of heteromer formation between GPCRs is still a large question in the field. Since the $D_{4.7}$ receptor variant has the longest 3IL and is the only polymorphic form not forming heteromers with the D_{2S} receptor, steric hindrance of the 3IL of $D_{4.7}$ receptor is a probable mechanism responsible for this lack of heteromerization, but other mechanisms cannot be ruled out. Using two-hybrid methodologies as well as proteomic studies, interactions between dopamine receptors and a cohort of dopamine receptor interacting proteins (DRIPs) have been demonstrated, forming signaling complexes or signalplexes.[25,26] Some of these DRIPs show selectivity for some dopamine receptor subtypes. For example, filamin or protein 4.1N interact with D_2 and D_3 receptors but not with D_1, D_5 or D_4 receptors,[27,28] the PDZ domain-containing protein, GIPC (GAIP interacting protein, C terminus) interacts with D_2 and D_3 receptor but not with the D_4 receptor subtype[29] and paralemmin interacts exclusively with D_3, but not with D_2 or D_4 receptors.[30] All of these interactions modulate receptor targeting, trafficking and signaling. Proline-rich sequences of the D_4 receptor, mainly located in the polymorphic region of the 3IL, constitute putative SH3 binding domains which can potentially interact with adapter proteins like Grb2 and Nck, which do not have any known catalytic activity but are capable of recruiting multiprotein complexes to the receptor.[24] It can be hypothetized that differences in DRIPs recruitment by $D_{4.7}$ and the other D_4 polymorphic forms can influence the $D_{4.7}$ ability to form heteromers, but future studies will be required.

Previous experiments indicated that locally in the striatum dopamine inhibits glutamate release by activating D_2 receptors (predominantly D_{2S}) localized in glutamatergic terminals.[13,23] Other studies also indicate that striatal postsynaptic D_2 receptors (predominantly D_{2L}) indirectly modulate glutamate release by retrograde endocannabinoids signaling.[31] The present results indicate that D_4 receptors also play a key role in the modulation of striatal glutamate release, likely through its ability to form heteromers with presynaptic D_{2S} receptors. In the striatal D_{2S}-D_4 receptor heteromer, low concentrations of dopamine should bind to the D_4 receptor, which has more affinity for dopamine than the D_{2S} receptor,[24] causing a certain degree of inhibition of glutamate release. However, at higher concentrations, dopamine should also bind to the D_{2S} receptor and under these conditions the synergistic interaction in the D_{2S}-D_4 receptor heteromer will produce an even stronger inhibition of glutamate release. Therefore, the D_{2S}-D_4 receptor heteromer seems to act as a concentration-dependent device that establishes two different degrees of presynaptic dopaminergic control over striatal glutamatergic neurotransmission. Since the strong modulation observed with higher concentrations of dopamine depends on D_{2S}-D_4 receptor heteromerization, the existence of a $D_{4.7}$ variant implies a weaker control of glutamatergic neurotransmission, which could be a main mechanism involved in the pathogenesis of ADHD. This could also explain at least part of the so far not understood successful effect of

psychostimulants in ADHD, which amplify dopaminergic signaling and these medications appear to be more effective in ADHD patients with the $D_{4.4}$ than with the $D_{4.7}$ variants.[32,33] We have to take into account that the existence of a $D_{4.7}$ variant does not imply ADHD is the result of this variant, but rather that it is one factor that contributes to its development. In fact, the $D_{4.7}$ variant might constitute a successful evolutionary trait under the appropriate environmental exposure.[7,34] The present study provides a new element of interest in the field of receptor heteromes, which now become new targets to be studied when dealing with functional differences associated with polymorphisms of G-protein-coupled receptor genes.

Supplementary Material

Refer to Web version on PubMed Central for supplementary material.

Acknowledgements

We thank the technical help from Jasmina Jiménez (University of Barcelona). Study supported by the NIDA IRP funds and from grants from Spanish Ministerio de Ciencia y Tecnología (SAF2008-03229-E, SAF2009-07276, SAF2010-18472, SAF2008-01462 and Consolider-Ingenio CSD2008-00005) and from Consejo Nacional de Ciencia y Tecnología de México (50428-M). P.J.M. is a Ramón y Cajal Fellow.

References

1. Lauzon NM, Laviolette SR. Dopamine D4-receptor modulation of cortical neuronal network activity and emotional processing: Implications for neuropsychiatric disorders. Behav Brain Res. 2010; 208:12–22. [PubMed: 19948192]
2. Tarazi FI, Campbell A, Yeghiayan SK, Baldessarini RJ. Localization of dopamine receptor subtypes in corpus striatum and nucleus accumbens septi of rat brain: comparison of D1-, D2-, and D4-like receptors. Neuroscience. 1998; 83:169–176. [PubMed: 9466407]
3. Svingos AL, Periasamy S, Pickel VM. Presynaptic dopamine D(4) receptor localization in the rat nucleus accumbens shell. Synapse. 2000; 36:222–232. [PubMed: 10819901]
4. LaHoste GJ, Swanson JM, Wigal SB, Glabe C, Wigal T, King N, et al. Dopamine D4 receptor gene polymorphism is associated with attention deficit hyperactivity disorder. Mol Psychiatry. 1996; 1:121–124. [PubMed: 9118321]
5. Swanson JM, Kinsbourne M, Nigg J, Lanphear B, Stefanos GA, Volkow N, et al. Etiologic subtypes of attention-deficit/hyperactivity disorder: barin imaging, molecular genetics and environmental factors and the dopamine hypothesis. Neuropsychol Rev. 2007; 17:39–59. [PubMed: 17318414]
6. Casey BJ, Nigg JT, Durston S. New potential leads in the biology and treatment of attention deficit-hyperactivity disorder. Curr Opin Neurol. 2007; 20:119–124. [PubMed: 17351480]
7. Wang E, Ding YC, Flodman P, Kidd JR, Kidd KK, Grady DL, et al. The genetic architecture of selection at the human dopamine receptor D4 (DRD4) gene locus. Am J Hum Genet. 2004; 74:931–944. [PubMed: 15077199]
8. Chang FM, Kidd JR, Livak KJ, Pakstis AJ, Kidd KK. The world-wide distribution of allele frequencies at the human dopamine D4 receptor locus. Hum Genet. 1996; 98:91–101. [PubMed: 8682515]
9. Asghari V, Sanyal S, Buchwaldt S, Paterson A, Jovanovic V, Van Tol HH. Modulation of intracellular cyclic AMP levels by different human dopamine D4 receptor variants. J Neurochem. 1995; 65:1157–1165. [PubMed: 7643093]
10. Ferré S, Baler R, Bouvier M, Caron MG, Devi LA, Durroux T, et al. Building a new conceptual framework for receptor heteromers. Nat Chem Biol. 2009; 5:131–134. [PubMed: 19219011]
11. Marcellino D, Ferré S, Casadó V, Cortés A, Le Foll B, Mazzola C, et al. Identification of dopamine D1-D3 receptor heteromers. Indications for a role of synergistic D1-D3 receptor interactions in the striatum. J Biol Chem. 2008; 283:26016–26025. [PubMed: 18644790]

12. Borroto-Escuela DO, Van Craenenbroeck K, Romero-Fernandez W, Guidolin D, Woods AS, Rivera A, et al. Dopamine D2 and D4 receptor heteromerization and its allosteric receptor-receptor interactions. Biochem Biophys Res Commun. 2011; 404:928–934. [PubMed: 21184734]
13. De Mei C, Ramos M, Iitaka C, Borrelli E. Getting specialized: presynaptic and postsynaptic dopamine D2 receptors. Curr Opin Pharmacol. 2009; 9:53–58. [PubMed: 19138563]
14. Carriba P, Navarro G, Ciruela F, Ferré S, Casadó V, Agnati L, et al. Detection of heteromerization of more than two proteins by sequential BRET-FRET. Nat Methods. 2008; 5:727–733. [PubMed: 18587404]
15. Pontieri FE, Tanda G, Di Chiara G. Intravenous cocaine, morphine, and amphetamine preferentially increase extracellular dopamine in the "shell" as compared with the "core" of the rat nucleus accumbens. Proc Natl Acad Sci USA. 1995; 92:12304–12308. [PubMed: 8618890]
16. Quarta D, Ferré S, Solinas M, You ZB, Hockemeyer J, Popoli P, et al. Opposite modulatory roles for adenosine A1 and A2A receptors on glutamate and dopamine release in the shell of the nucleus accumbens. Effects of chronic caffeine exposure. J Neurochem. 2004; 88:1151–1158. [PubMed: 15009670]
17. Garcia M, Floran B, Arias-Montaño JA, Young JM, Aceves J. Histamine H3 receptor activation selectively inhibits dopamine D1 receptor-dependent [3H]GABA release from depolarization-stimulated slices of rat substantia nigra pars reticulata. Neuroscience. 1997; 80:241–249. [PubMed: 9252235]
18. Cortés H, Paz F, Erlij D, Aceves J, Florán B. GABA(B) receptors modulate depolarization-stimulated [^{3}H]glutamate release in slices of the pars reticulata of the rat substantia nigra. Eur J Pharmacol. 2010; 649:161–167. [PubMed: 20863782]
19. Powell SB, Paulus MP, Hartman DS, Godel T, Geyer MA. RO-10-5824 is a selective dopamine D4 receptor agonist that increases novel object exploration in C57 mice. Neuropharmacology. 2003; 44:473–481. [PubMed: 12646284]
20. Gackenheimer SL, Schaus JM, Gehlert DR. [3H]-quinelorane binds to D2 and D3 dopamine receptors in the rat brain. J Pharmacol Exp Ther. 1995; 274:1558–1565. [PubMed: 7562534]
21. Thomas TC, Kruzich PJ, Joyce BM, Gash CR, Suchland K, Surgener SP, et al. Dopamine D4 receptor knockout mice exhibit neurochemical changes consistent with decreased dopamine release. J Neurosci Meth. 2007; 166:306–314.
22. Thomas TC, Grandy DK, Gerhardt GA, Glaser PE. Decreased dopamine D4 receptor expression increases extracellular glutamate and alters its regulation in mouse striatum. Neuropsychopharmacology. 2008; 34:436–445. [PubMed: 18536704]
23. Bamford NS, Zhang H, Schmitz Y, Wu NP, Cepeda C, Levine SM, et al. Heterosynaptic dopamine neurotransmission selects sets of corticostriatal terminals. Neuron. 2004; 42:653–663. [PubMed: 15157425]
24. Rondou P, Haegeman G, Van Craenenbroeck K. The dopamine D4 receptor: biochemical and signalling properties. Cell Mol Life Sci. 2010; 67:1971–1986. [PubMed: 20165900]
25. Kabbani N, Levenson R. A proteomic approach to receptor signaling: molecular mechanisms and therapeutic implications derived from discovery of the dopamine D2 receptor signalplex. Eur J Pharmacol. 2007; 572:83–93. [PubMed: 17662712]
26. Yao WD, Spealman RD, Zhang J. Dopaminergic signaling in dendritic spines. Biochem Pharmacol. 2008; 75:2055–2069. [PubMed: 18353279]
27. Lin R, Karpa K, Kabbani N, Goldman-Rakic P, Levenson R. Dopamine D2 and D3 receptors are linked to the actin cytoskeleton via interaction with filamin A. Proc Natl Acad Sci USA. 2001; 98:5258–5263. [PubMed: 11320256]
28. Binda AV, Kabbani N, Lin R, Levenson R. D2 and D3 dopamine receptor cell surface localization mediated by interaction with protein 4.1N. Mol Pharmacol. 2002; 62:507–513. [PubMed: 12181426]
29. Jeanneteau F, Diaz J, Sokoloff P, Griffon N. Interactions of GIPC with dopamine D2, D3 but not D4 receptors define a novel mode of regulation of G protein-coupled receptors. Mol Biol Cell. 2004; 15:696–705. [PubMed: 14617818]

30. Basile M, Lin R, Kabbani N, Karpa K, Kilimann M, Simpson I, Kester M. Paralemmin interacts with D3 dopamine receptors: implications for membrane localization and cAMP signaling. Arch Biochem Biophys. 2006; 446:60–68. [PubMed: 16386234]

31. Yin HH, Lovinger DM. Frequency-specific and D2 receptor-mediated inhibition of glutamate release by retrograde endocannabinoid signaling. Proc Natl Acad Sci USA. 2006; 103:8251–8256. [PubMed: 16698932]

32. Cheon KA, Kim BN, Cho SC. Association of 4-repeat allele of the dopamine D4 receptor gene exon III polymorphism and response to methylphenidate treatment in Korean ADHD children. Neuropsychopharmacology. 2007; 32:1377–1383. [PubMed: 17077808]

33. Hamarman S, Fossella J, Ulger C, Brimacombe M, Dermody J. Dopamine receptor 4 (DRD4) 7-repeat allele predicts methylphenidate dose response in children with attention-deficit/hyperactivity disorder: a pharmacogenetic study. J Child Adolesc Psychopharmacol. 2004; 14:564–574. [PubMed: 15662148]

34. Ding YC, Chi HC, Grady DL, Morishima A, Kidd JR, Kidd KK, et al. Evidence of positive selection acting at the human dopamine receptor D4 gene locus. Proc Natl Acad Sci USA. 2002; 99:309–314. [PubMed: 11756666]

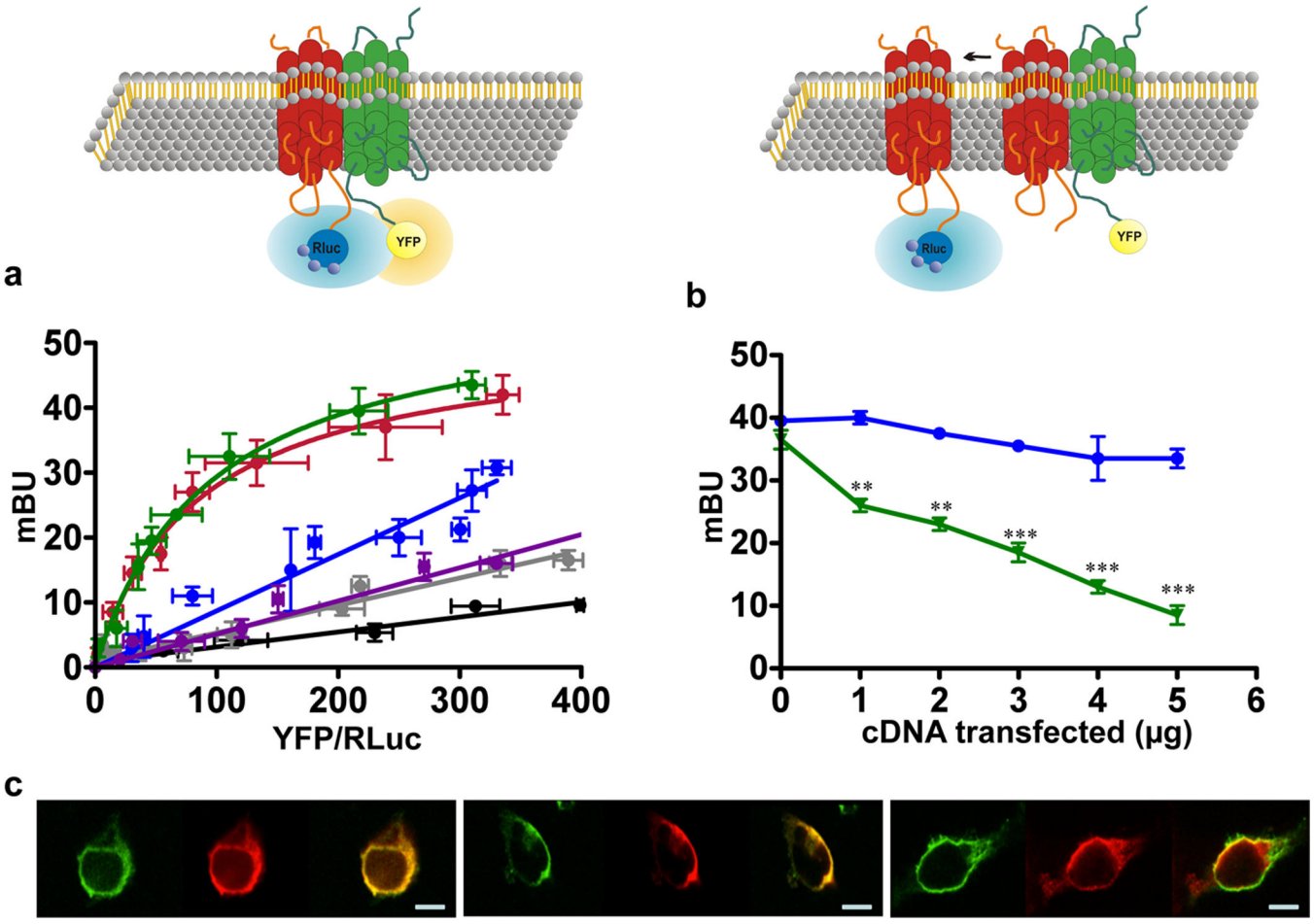

Figure 1. Human D_{2S} and D_4 receptors form heteromers in transfected cells

a) BRET saturation curves were obtained from experiments with cells co-expressing, top to bottom, D_{2S}-YFP and $D_{4.2}$-RLuc (red), $D_{4.4}$-RLuc (green) or $D_{4.7}$-Rluc (blue), D_{2S}-RLuc and $D_{4.7}$-YFP (purple), A_1-RLuc and D_{2S}-YFP (black) or $D_{4.4}$-RLuc and D_1-YFP (gray). Co-transfections were performed with a constant amount of cDNA corresponding to the receptor-RLuc construct (2 μg of cDNA for D_4-RLuc or 1 μg of cDNA for A_1-RLuc) and increasing amounts of cDNA corresponding to the receptor-YFP construct (0.2–6 μg of cDNA for D_{2S}-YFP or 1–4 μg of cDNA for D_1-YFP). Both fluorescence and luminescence of each sample were measured prior to every experiment to confirm equal expression of Rluc (about 100,000 luminescence units) while monitoring the increase of YFP expression (2000 to 20,000 fluorescence units). BRET data are expressed as means ± S.D. of four to nine different experiments grouped as a function of the amount of BRET acceptor. (**b**) BRET displacement experiments were performed in cells expressing constant amounts of $D_{4.4}$-RLuc (2 μg cDNA transfected) and D_{2S}-YFP (2μg cDNA tranfected) and increasing amounts (1–5 μg of cDNA transfected) of $D_{4.7}$ (blue) or $D_{4.2}$ (green). Both fluorescence and luminescence of each sample were measured prior to every experiment to confirm no changes in the expression of $D_{4.4}$-RLuc and D_{2S}-YFP. BRET data are expressed as means ± S.D. of five different experiments grouped as a function of the amount of BRET acceptor. Significant differences with respect to the samples without $D_{4.2}$ or $D_{4.7}$ were calculated by

one-way ANOVA and Bonferroni's test. (**$P < 0.01$ and ***$P < 0.001$). In **(a)** and **(b)** the relative amounts of BRET acceptor are expressed as the ratio between the fluorescence of the acceptor minus the fluorescence detected in cells only expressing the donor, and the luciferase activity of the donor. In the top, schematic representations of BRET **(a)** or BRET displacement **(b)** are shown. **(c)** Confocal microscopy images of cells transfected with 1 μg of cDNA corresponding to, left to right, $D_{4.2}$-RLuc, $D_{4.4}$-RLuc or $D_{4.7}$-RLuc and 0.5 μg cDNA corresponding to D_{2S}-YFP. Proteins were identified by fluorescence or by immunocytochemistry. D_4-RLuc receptors are shown in red, D_{2S}-YFP is shown in green and co-localization is shown in yellow. Scale bar: 5 μm.

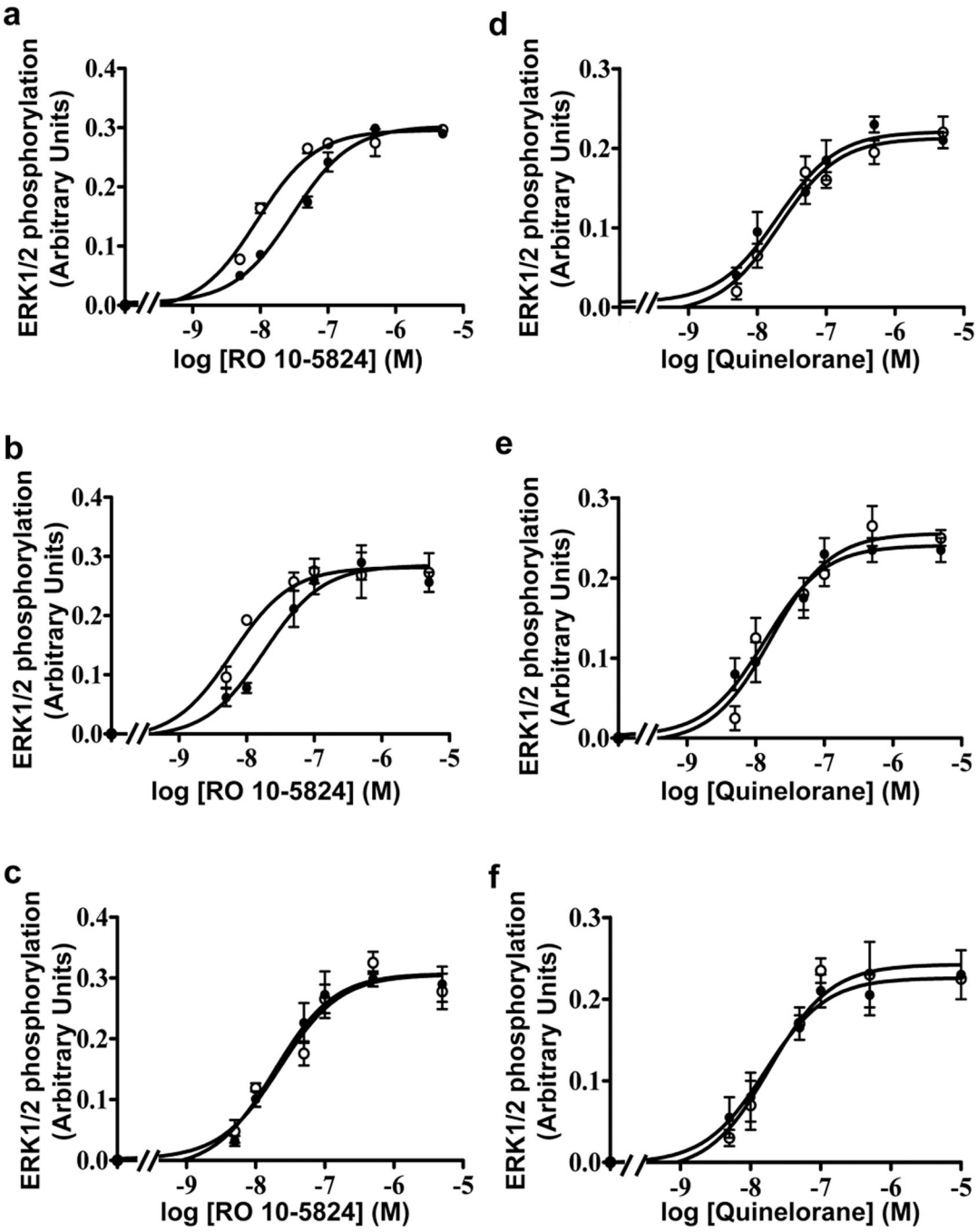

Figure 2. Crosstalk between human D_4 and D_{2S} receptors in ERK 1/2 phosphorylation

Cells were transiently co-transfected with 2.5 μg of cDNA corresponding to D_{2S} and 2.5 μg of cDNA corresponding to $D_{4.2}$ (**a** and **d**), $D_{4.4}$ (**b** and **e**) or $D_{4.7}$ (**c** and **f**). In **a**, **b** and **c**, cells were treated for 10 min with increasing concentrations of RO 10-5824 in the presence (○) or in the absence (●) of quinelorane (50 nM). In **d, e** and **f,** cells were treated for 10 min with increasing concentrations of quinelorane in the presence (○) or in the absence (●) of RO 10-5824 (50 nM). The immunoreactive bands, corresponding to ERK 1/2 phosphorylation, of three to six experiments were quantified and expressed as arbitrary

units. For each curve EC_{50} values were calculated as mean ± S.E.M. and statistical differences between curves obtained in the presence or in the absence of quinelorane (**a, b** and **c**) or RO 10-5824 (**d, e** and **f**) were determined by Student's *t* test. EC_{50} with and without quinelorane: **(a)** 9 ± 1 and 26 ± 1nM ($p<0.01$), **(b)** 7 ± 1 and 23 ± 1nM ($p<0.01$), **(c)** 18 ± 1 and 22 ± 1 nM (N.S.). EC_{50} with and without RO 10-5824: **(d)** 22 ± 1 and 20 ± 1 nM (N.S.), **(e)** 20 ± 1 and 17 ± 1 nM (N.S.), **(f)** 18 ± 1 and 13 ± 1nM (N.S.). N.S.: non-statistical differences

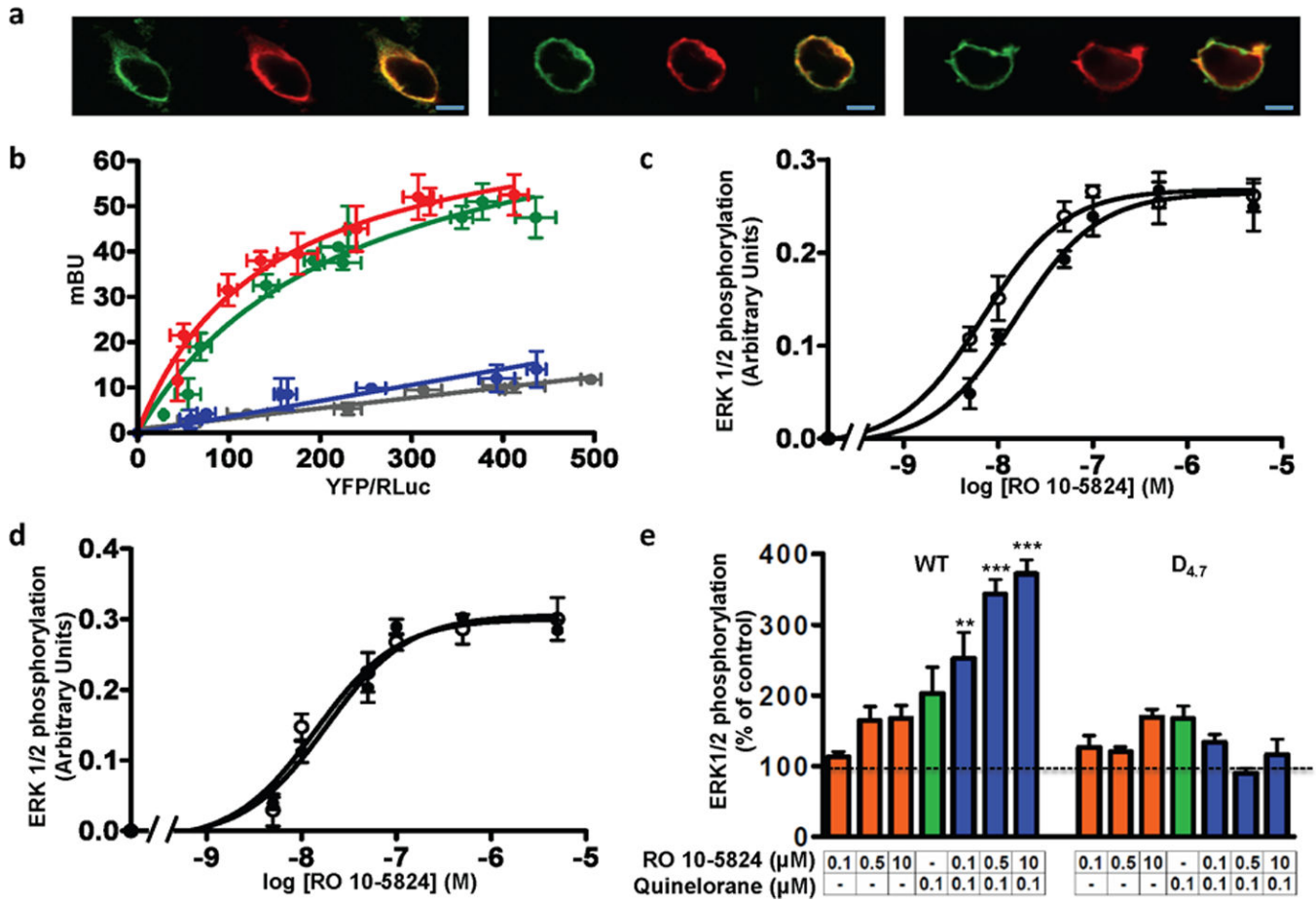

Figure 3. D_{2S}-D_4 receptor heteromers in the mouse brain

(a) Confocal microscopy images of cells transfected with 1 μg of cDNA corresponding to, left to right, mouse D_4-RLuc, human $D_{4.4}$-RLuc and human $D_{4.7}$-RLuc and 0.5 μg of cDNA corresponding to D_{2S}-YFP. Proteins were identified by fluorescence or by immunocytochemistry. D_4-RLuc receptors are shown in red, D_{2S}-YFP is shown in green and co-localization is shown in yellow. Scale bar: 5 μm. **(b)** Mouse D_{2S} receptor heteromerization with mouse and human D_4 receptors. BRET saturation curves were obtained from cells co-expressing mouse D_4-Rluc (green), human $D_{4.4}$-RLuc (red), human $D_{4.7}$-RLuc (blue) or human A_1-RLuc (gray) and mouse D_{2S}-YFP receptors. Co-transfections were performed with a constant amount of cDNA corresponding to the receptor-RLuc construct (2 μg of cDNA for mouse D_4-RLuc, 2.5 μg of cDNA for human D_4-RLuc or 1 μg of cDNA for A_1-RLuc) and increasing amounts of cDNA corresponding to the receptor-YFP construct (0.2–6 μg cDNA). Both fluorescence and luminescence of each sample were measured prior to every experiment to confirm equal expression of Rluc (about 100,000 luminescence units) while monitoring the increase of YFP expression (2000 to 20,000 fluorescence units). The relative amounts of BRET acceptor are expressed as the ratio between the fluorescence of the acceptor minus the fluorescence detected in cells only expressing the donor, and the luciferase activity of the donor. BRET data are expressed as means ± S.D. of three to six different experiments grouped as a function of the amount of BRET acceptor. **(c)** and **(d)** Crosstalk between mouse D_{2S} receptors and mouse or human D_4

receptors in ERK 1/2 phosphorylation. Cells transiently co-expressing mouse D_{2S} receptors and mouse D_4 receptors (**c**) or human $D_{4.7}$ receptors (**d**) were treated for 10 minutes with increasing RO 10-5824 concentrations in the presence (○) or in the absence (●) of quinelorane (50 nM) prior to the ERK 1/2 phosphorylation determination. The immunoreactive bands of three experiments (mean ± SEM; $n = 3$) were quantified and expressed as arbitrary units. EC_{50} values with or without quinelorane were: (c) 7 ± 0.1 and 15 ± 0.1 nM (Student's *t* test: $p<0.01$) or **(d)** 18 ± 0.1 and 15 ± 0.1 nM (Student's *t* test: NS). **(e)** Striatal slices from wild-type (WT) or $D_{4.7}$ mutant mice were treated for 10 min with the indicated concentrations of RO 10-5824 (orange) or quinelorane (green) or with RO 10-5824 plus quinelorane (blue) and ERK 1/2 phosphorylation was determined. For each treatment, the immunoreactive bands from 4 to 6 slices from a total 10 WT and 10 $D_{4.7}$ mutant animals were quantified and values represent the mean ± S.E.M. of the percentage of phosphorylation relative to basal levels found in untreated slices (100 %). No significant differences were obtained between the basal levels of the WT and the $D_{4.7}$ mutant mice. Significant treatment and genotype effects were shown by a bifactorial ANOVA followed by post-hoc Bonferroni's tests (** and ***: $p<0.01$ and $p<0.001$, respectively, as compared to the lowest concentration of RO 10-5824)

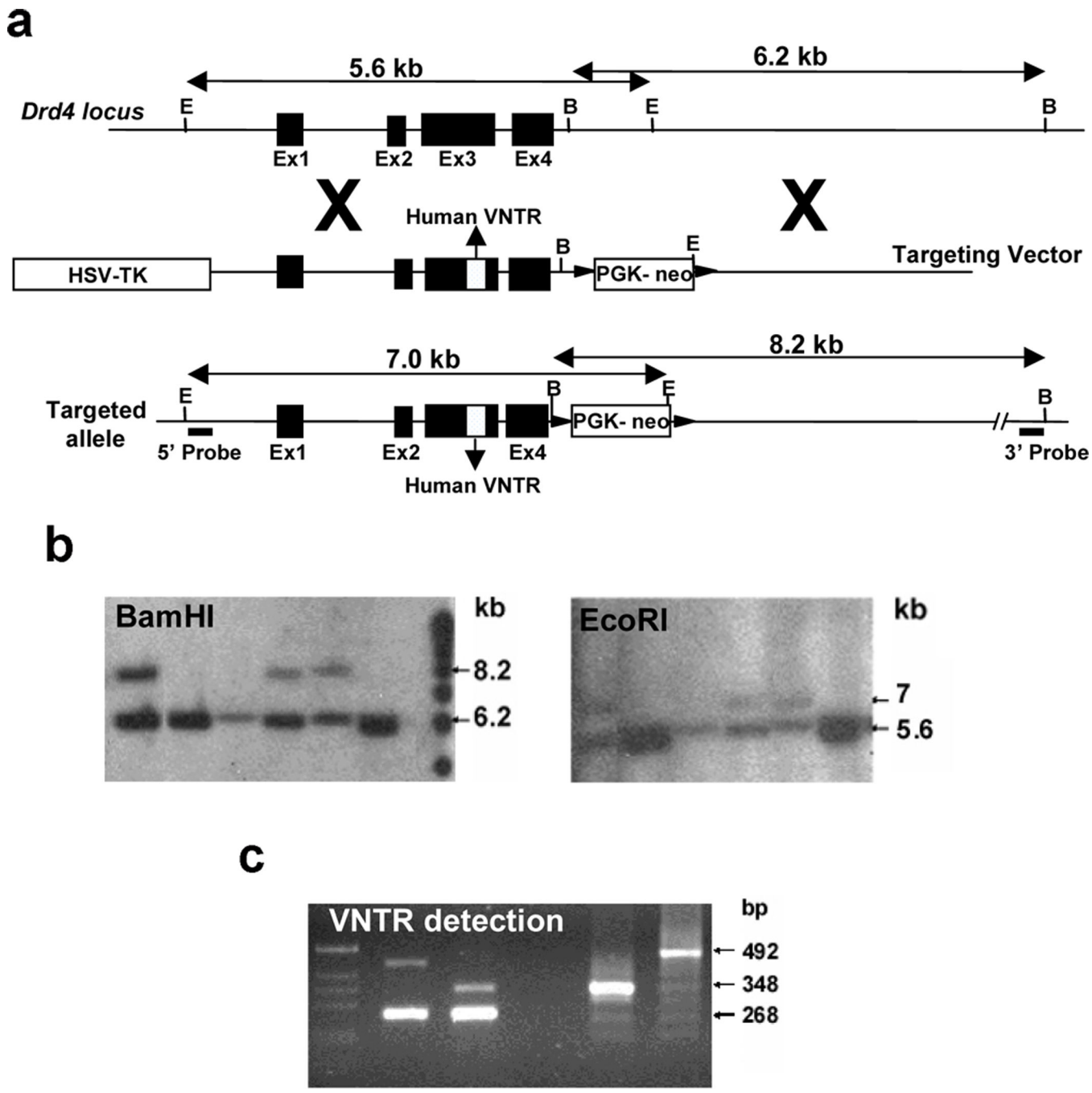

Figure 4. Targeted insertion of human VNTRs carrying 7 repeats into the mouse *Drd4* exon 3 by homologous recombination in ES cells

(a) Structure of the *Drd4 locus*, targeting vector and targeted allele. **(b)** Southern blot analysis detected double homologous recombination events at the 5' and 3' ends using external probes after digestion with BamHI or EcoRI. **(c)** The presence of inserted human VNTR was verified by PCR using mouse primers flanking the expansion.

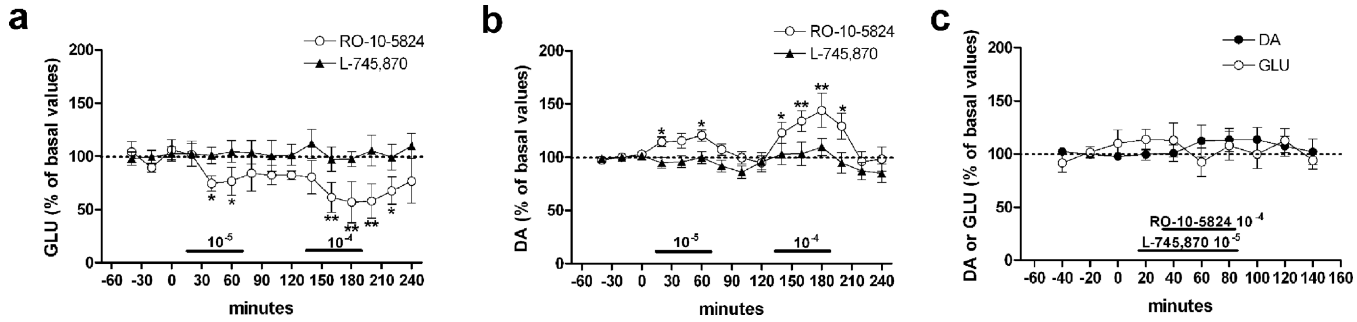

Figure 5. ***In vivo*** **D_4 receptor-mediated modulation of basal extracellular levels of glutamate in the rat ventral striatum**

Effects of the local perfusion with the D_4 receptor agonist RO 10-5824 and the D_4 receptor antagonist L-745,870 on the basal extracellular concentrations of glutamate (GLU) and dopamine (DA) in the ventral striatum (core of the nucleus accumbens). Horizontal bars show the periods of drug perfusion (concentrations are indicated in M). Data represent means ± S.E.M. of the percentage of the mean of the three basal values before the first drug perfusion (n = 6–8/group): * and **: $p<0.05$ and 0.01, respectively, compared to the values previous in time “0” (repeated measures ANOVA followed by Newman-Keuls tests).

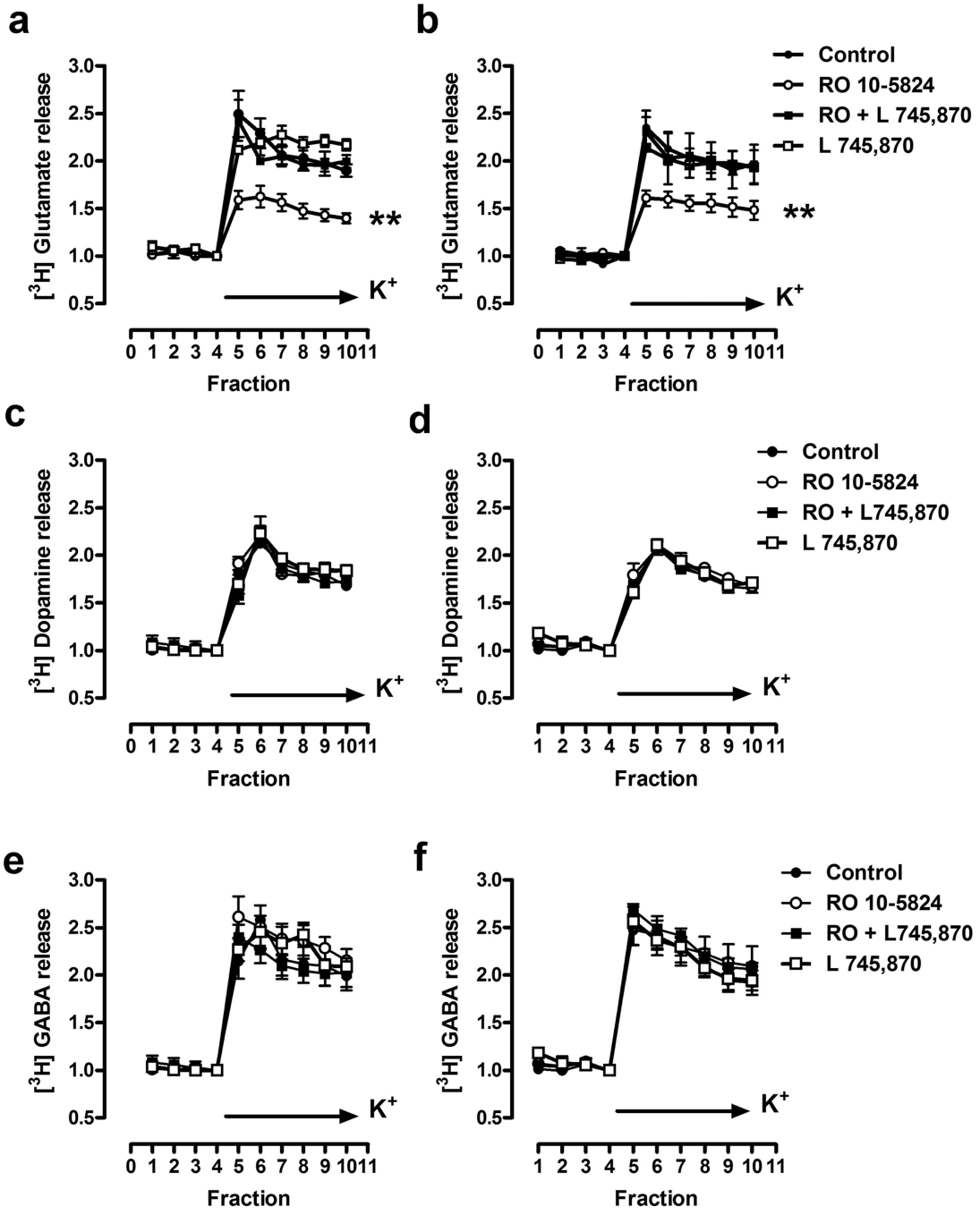

Figure 6. D_4 receptor-mediated modulation of [^{3}H]glutamate, but not [^{3}H]dopamine or [^{3}H]GABA release from slices of dorsal and ventral striatum

Slices from the dorsal striatum (caudate-putamen; **a, c** and **e)** or the ventral striatum (nucleus accumbens; **b, d** and **f**) of reserpine-treated rats were treated with the D_4 receptor agonist RO 10-5824 (100 nM) or with the D_4 receptor antagonist L745,870 (10 nM) alone or in combination and the time course of K^+ stimulated [^{3}H]glutamate (**a** and **b**), [^{3}H]dopamine (**c** and **d**) or [^{3}H]GABA (**e** and **f**) release was determined. The RO 10-5824-induced effect (open circles) was prevented by the antagonist L 745,870 (dark squares) which itself had no

effect (open squares). Values are mean ± S.E.M. of samples from 3 different animals performed in 4 replicates. Drug effect was assessed by comparing the relative area under the curve for each condition. **: $p<0.01$ with respect to the control (ANOVA followed by Tukey-Kramer multiple comparison post hoc test).

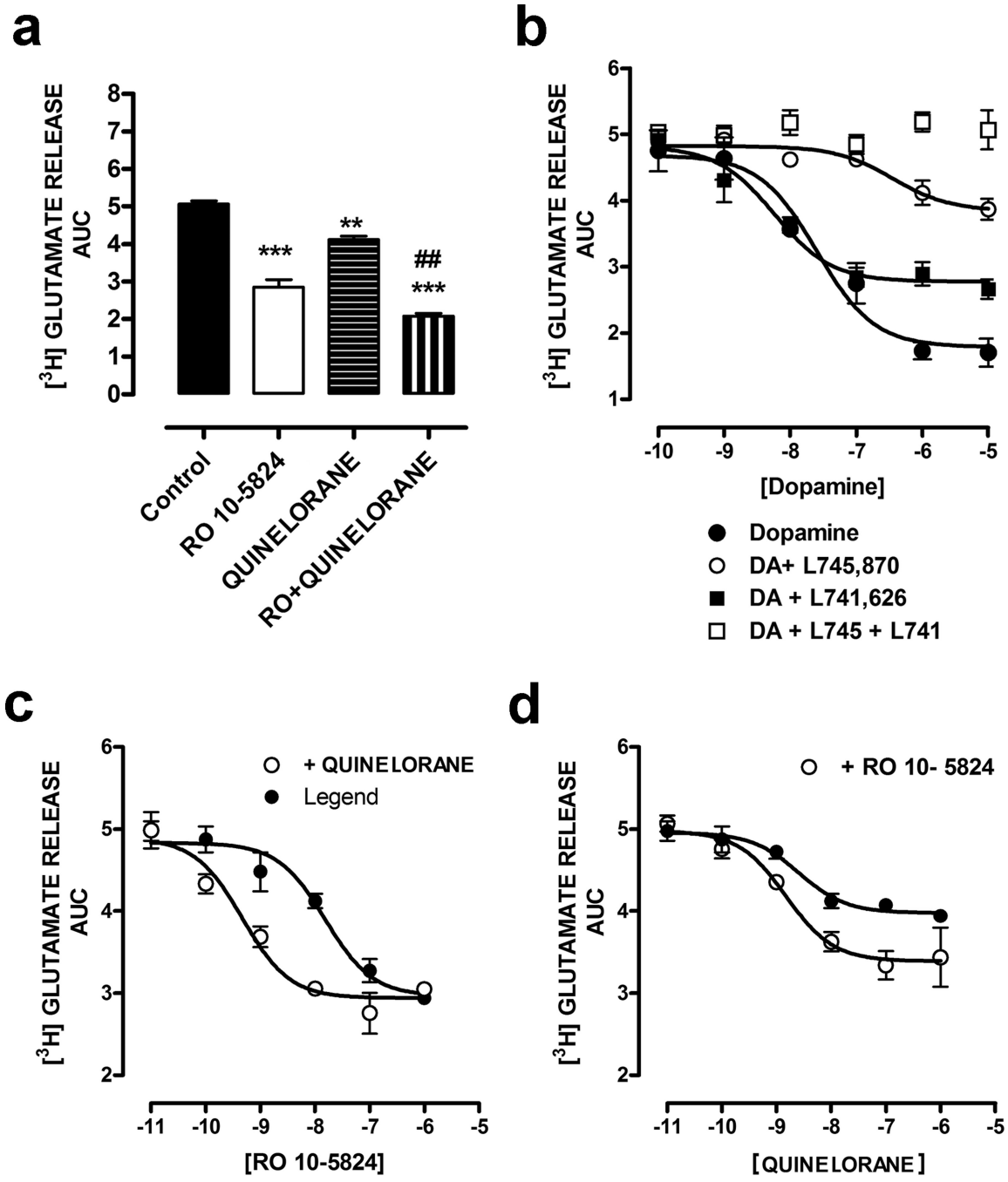

Figure 7. D_2 and D_4 receptor interactions in the modulation of striatal [^{3}H]glutamate release

Striatal slices (dorsal striatum) from reserpine-treated rats were incubated with SCH 23390 (100 nM) to block D_1 receptor activation. In (**a**), slices were treated for 32 min (fraction 2 to fraction 10) with medium (control), with the D_4 receptor agonist RO 10-5824 (100 nM), with the $D_{2/3}$ receptor agonist quinelorane (100 nM) or with both and K^+ stimulated [^{3}H]glutamate release was determined. Values are mean ± S.E.M. of samples from 3 different animals performed in 4 replicates. Drug effects were assessed by comparing the relative area under the curve for each condition. **p<0.01 and ***p<0.001 with respect to

the control and ## p<0.01 with respect to slices treated with RO 10-5824 or quinelorane alone (ANOVA followed by Tukey-Kramer multiple comparison post hoc test). In (**b**), slices were treated for 32 min with increasing dopamine concentrations in absence (dark circles) or in the presence of the D_4 receptor antagonist L-45,870 (10 nM, dark squares), the D_2 receptor antagonist L 741,626 (10 nM, open circles) or both (open squares) and K^+ stimulated [^{3}H]glutamate release was determined. Values are mean ± S.E.M. of samples from 3 different animals performed in 4 replicates. Drug effects were assessed by comparing the relative area under the curve for each condition. The IC_{50} values were: 25.25 nM (C.I.: 9.63–66.20 nM) for dopamine alone, 5.75 nM (2.12–15 nM) for dopamine in the presence of L-741,626 and 357.27 nM (C.I.: 73.40–1739 nM) for dopamine in the presence of L 745,870. In **(c)** slices were treated for 32 min with increasing concentrations of RO 10-5824 in the absence (black circles) or in the presence (open circles) of quinelorane (10 nM) and K^+ stimulated [^{3}H]glutamate release was determined. In **(d)** slices were treated for 32 min with increasing concentrations of quinelorane in the absence (black circles) or in the presence (open circles) of RO 10-5824 (10 nM) and K^+ stimulated [^{3}H]glutamate release was determined. In **(c)** and **(d)**, values are mean ± S.E.M. of samples from 3 different animals performed in 4 replicates. The IC_{50} values were: (**c**) 15 nM (35.15-6.55 nM) for RO 10-5824 alone and 0.05 nM (1.21-0.02 nM) for RO 10-5824 in the presence of quinelorane (Student's *t* test: p<0.01) and (**d**) 2.55 nM (7.31-0.89 nM) for quinelorane alone and 1.48 nM (4.5-0.45 nM) for quinelorane in the presence of RO 10-5824 (Student's *t* test; NS).